DISTRIBUTION STATEMENT A: Approved for public release; distribution is unlimited.

Propagation and Ambient Noise Studies for Ocean Acoustics Applications

Martin Siderius
Portland State University, ECE Department
1900 SW 4th Ave., Portland, OR 97201
phone:(503) 725-3223 fax:(503) 725-3807 email: siderius@pdx.edu

Award Number: N000140910238
http://www.ece.pdx.edu/Faculty/Siderius.php

LONG-TERM GOALS

The objective of this research is to study the characteristics of the low and mid frequency ocean ambient noise field. This is in combination with studying how to develop physics based processing to improve sonar system performance in low signal to noise ratio scenarios.

OBJECTIVES

Basic research on ocean ambient noise has led to several potential applications for the Navy. In recent work we have developed a new type of passive sensor that uses ocean noise to extract information about the seabed properties without using sound projectors or explosives [1]. The value and impact of these techniques could be significant and we are investigating various ways to take advantage of the noise field. The passive nature of noise based processing is appealing in situations where sound sources are not desired (*e.g.* due to environmental restrictions). Further, the measurements are relatively simple compared to using conventional methods which require one (possibly two) research ship(s) as well as specialized sources and/or sonar systems (*e.g.* chirp sonar). While the noise processing techniques are a powerful tool for passive seabed-characterization, we are just beginning to understand how these methods work as well as the limitations.

APPROACH

The work focuses on estimating the physical parameters of the bottom by processing ocean ambient noise. Two passive techniques are under development/investigation: The passive fathometer [1] and the estimation of the bottom loss by beam forming (BF) the noise field [2].

EXTRACTION OF THE NORMAL INCIDENCE RAYLEIGH REFLECTION COEFFICIENT FROM THE PASSIVE FATHOMETER OUTPUT

The *passive fathometer* (PF), is a technique that can produce a vertical profile of the seabed using only naturally-occurring acoustic sources (*i.e.*, noise from rain, breaking waves, and wind at the sea surface) [1]. This year we have developed a method that uses the passive-fathometer output for estimating the normal-incidence Rayleigh reflection coefficient (RRC). The time-domain RRC reveals information about the seabed layers and their reflectivity (which is related to the sound speed and density of the layer). This is accomplished by time-gating the output together with applying a scaling factor that is determined by using an incoherent estimate of the total power loss. In order to determine the

appropriate time-gate range, it was necessary to develop a model that ultimately provided a closed-form approximation to the passive-fathometer output (see publication [1] for the details).

GEOACOUSTIC INVERSION THROUGH BOTTOM-LOSS ESTIMATE USING AMBIENT NOISE

Use of the *minimum-variance distortionless-response* (MVDR) beamformer significantly improved the imaging of seabed layers for the PF application (see publication [1]), and some authors have reported [3] or suggested [4] that use of adaptive beamforming techniques can improve ambient-noise inversion results (the claim in [3] is actually restricted to grazing angles below the critical angle). The potential for higher angular resolution with adaptive methods may provide improved estimates of the critical angle as well as better defined interference patterns seen in bottom loss curves from layered seabeds. In the work described here, the feasibility of applying the MVDR beamformer for geoacoustic inversion of ocean ambient noise has been investigated. The bottom loss (BL) is defined by the formula:

$$BL = -10Log\left|R\right|^2, \tag{1}$$

where R is the Rayleigh reflection loss. A technique for estimating BL as a function of grazing angle θ and frequency f from ambient noise data has been proposed [2] that is based on the estimate of the power reflection coefficient given by:

$$\left|\hat{R}(\theta_0,f)\right|^2 = \frac{B(-\theta_0,f)}{B(\theta_0,f)}. \tag{2}$$

where $B(\theta,f)$ is the beamformer output power when the array is steered towards direction $\phi = \theta$:

$$B(\phi,f) = \tilde{\mathbf{w}}^H \mathbf{p}(\tilde{\mathbf{w}}^H \mathbf{p})^H = \tilde{\mathbf{w}}^H \mathbf{K}\tilde{\mathbf{w}}. \tag{3}$$

In (3), H denotes the conjugate transpose operation, $\tilde{\mathbf{w}}(\phi,f) = [w_0, w_1, ..., w_{M-1}]^T$ is the weight vector for the beamforming steering angle ϕ (T denotes the transpose operation), $\mathbf{p}(f) = [p_1, p_2, ..., p_M]^T$ is the pressure data for each of the M hydrophones at a specific frequency f, and $\mathbf{K}(f) = \mathbf{p}\mathbf{p}^H$ is the cross spectral density (CSD) matrix at that same frequency, obtained by averaging multiple data segments. The bottom-loss estimate $\hat{BL}$ is obtained with,

$$\hat{BL} = -10Log\left|\hat{R}\right|^2. \tag{4}$$

The approach to investigating the application of MVDR to ambient noise based estimates of bottom loss and geo-acoustic inversion is based on both measured data analysis and simulations. The measured data results motivate the questions while the simulations provide a way to control the variables for a systematic investigation of the causes of anomalous results observed.

WORK COMPLETED

A model has been implemented and validated for computing the theoretical Rayleigh reflection coefficient (RRC) of a layered seabed. A technique has been developed to estimate the normal-incidence RRC using the passive fathometer technique. This has so far been validated numerically

through simulations using the OASN tool based on the OASES propagation codes [6] with details of the results in publication [3] and summarized in the next sections.

The application of adaptive beamforming techniques to the estimate of the reflection loss from marine ambient noise has been investigated. For comparison, both conventional and adaptive beamforming techniques were analyzed and applied to a dataset from the NATO Undersea Research Centre's Boundary 2003 experiment. Further, these methods were compared using simulated noise fields produced with OASN. Details of the analysis and results are provided in publication [4] and summarized in the next sections.

RESULTS

EXTRACTION OF THE NORMAL INCIDENCE RAYLEIGH REFLECTION COEFFICIENT FROM THE PASSIVE FATHOMETER OUTPUT

Figure 1 shows a comparison between a simple model for the PF output along with PF output generated by a full simulation where the noise field was produced using OASN [6] (the seabed geoacoustic parameters are given in Table 1). The simple model allows various beamforming effects on PF processing to be studied.

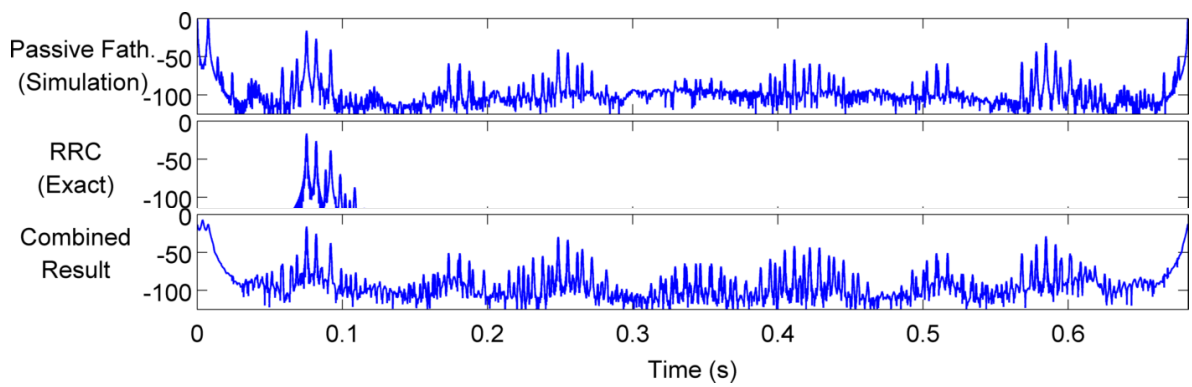

Figure 1: Top panel shows results of the passive fathometer output based on a simulation of the noise field using OASN followed by passive fathometer processing. The second panel from the top shows the exact Rayleigh reflection coefficient at normal incidence. The third panel is the result from an idealized model of the passive fathometer and accounts for beamformer effects. The model captures the main features of the passive fathometer output. Note, the large dynamic range of more than 100 dB on the vertical axis.

By correctly predicting the time span of the big artifact at the beginning of the RRC time series (in Fig. 1), the closed-form expression for the PF output affords the determination of a proper time-gate range, which combined with an estimate of the power reflection coefficient from measured data (see the bottom-loss estimate technique illustrated above), makes it possible to obtain an estimate of the RRC (on a meaningful dB scale) for the bottom using only ambient-noise data. Fig.2 shows excellent agreement between the simulated and estimated RRC in this case.

Table 1. Bottom configuration for the results shown inFig.2

	Thickness (m)	Sound Speed (m/s)	Density (kg/m^3)	Attenuation (dB/m)
Vacuum	Inf	0	0	0
Water	100	1500	1000	0
Sediment 1	5	1600	1500	0.14
Sediment 2	21.5	1700	1600	0.15
Sediment 3	Inf	1800	1800	0.15

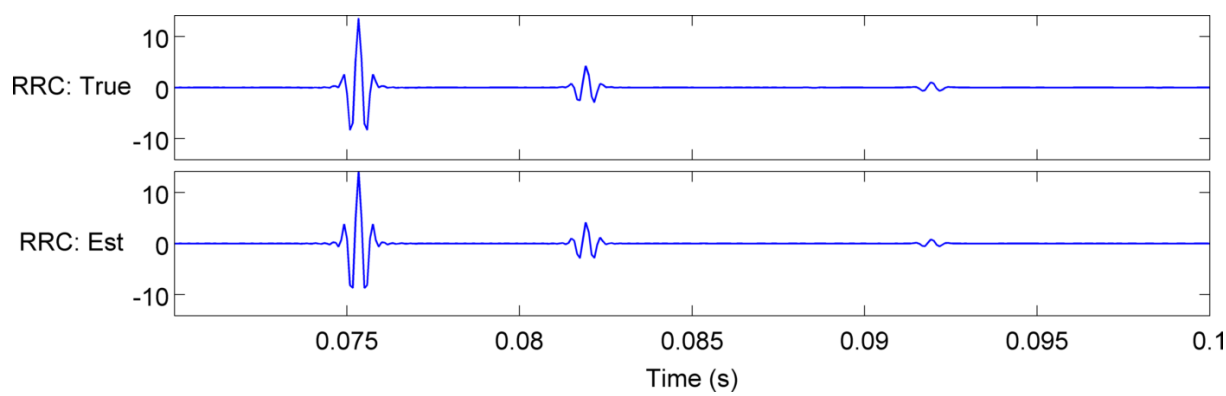

Figure 2: Comparison of the exact time-domain RRC (top panel) and the RRC estimated from noise (bottom panel). The vertical axis is in reflection coefficient and time is along the horizontal axis. The lines in the two panels are nearly indistinguishable.

GEOACOUSTIC INVERSION THROUGH BOTTOM-LOSS ESTIMATE

Following the technique outlined in eqs. (1)-(4), the bottom-loss estimate $\hat{BL}$ is obtained by replacing R with $\hat{R}$ as was done in eq. (4). An example of the results is shown in the left panel of Fig.3 in the form of what is called in this report a "BL *pattern*" (noise data provided from the NATO Undersea Research Centre's Boundary 2003 experiment [5]).

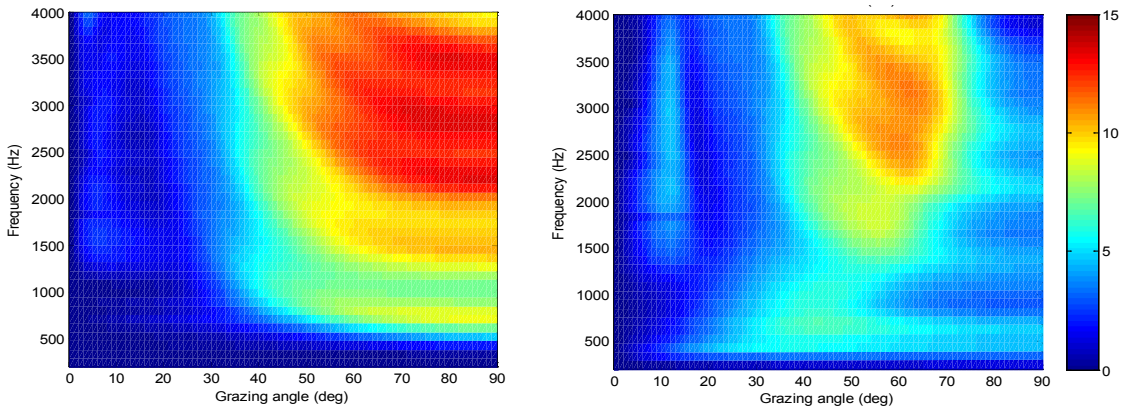

Figure 3: Reflection-loss pattern obtained by applying equations (2)-(4) to ocean ambient noise data collected from a drifting vertical line array. On the left is the bottom loss estimate using conventional beamforming. On the right is the estimate using MVDR. The low losses in the MVDR result at high grazing angles are not physically reasonable.

In eq. (3), the steering vector $\tilde{\mathbf{w}}$ can be computed using *conventional* BF (CBF) — this steering vector is usually denoted by **w** and each element of the vector is given by:

$$w_m(\phi, f) = e^{-imkd\sin\phi}, \tag{5}$$

or using *adaptive* BF techniques, such as the MVDR beam former:

$$\mathbf{w}_{MV}(\phi, f) = \frac{\mathbf{K}^{-1}\mathbf{w}}{\mathbf{w}^H\mathbf{K}^{-1}\mathbf{w}}. \tag{6}$$

Equation (6) is obtained as the solution to the minimization problem:

$$\underset{\mathbf{w}_{MV}}{\text{Min}}\ \mathbf{w}_{MV}^H\mathbf{K}\mathbf{w}_{MV} \text{ subject to } \mathbf{w}_{MV}^H\mathbf{w} = 1, \tag{7}$$

which shows that the MVDR beamformer attempts to minimize the contribution to the total power from noise and sources coming from directions different from ϕ, while maintaining a fixed gain in the look direction ϕ. Direct application of the MVDR beamformer to the Boundary 2003 data produced significant artifacts in the BL pattern, as shown in the right panel of Fig.3. The reason for this poor performance was investigated through simulation by applying the BF algorithms to CSD matrices produced by OASN (from the OASES package [6]) for bottom configurations ranging from simple half spaces to complex multi-layered seabeds. Since significant artifacts were observed in the same frequency/grazing angle regimes in the BL patterns obtained using synthesized data, it was possible to exclude the possibility that the artifacts could be due to array mismatch. Diagonal loading was used to stabilize the CSD matrices with respect to inversion, but artifacts were still present even at frequencies where numerical instability could be safely excluded. A "baseline" case was then developed, using a model that can output the CSD matrices due to a noise field interacting with a bottom having a

reflection coefficient that is independent of both frequency and grazing angle — in this case, the BL should have the same value (given by eq.(4)) over the entire BL pattern. Figure 4 shows that the artifacts are still present when using the MVDR beam former.

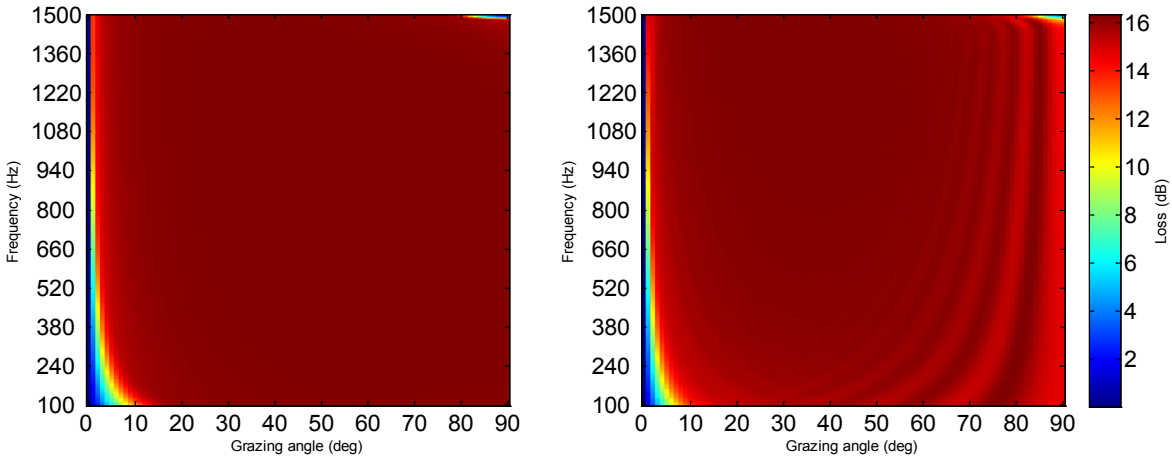

Figure 4: Bottom Loss patterns for the constant bottom loss case (constant over grazing angle and frequency). In the left panel the conventional beamforming result is shown and the MVDR beamformer result is on the right.

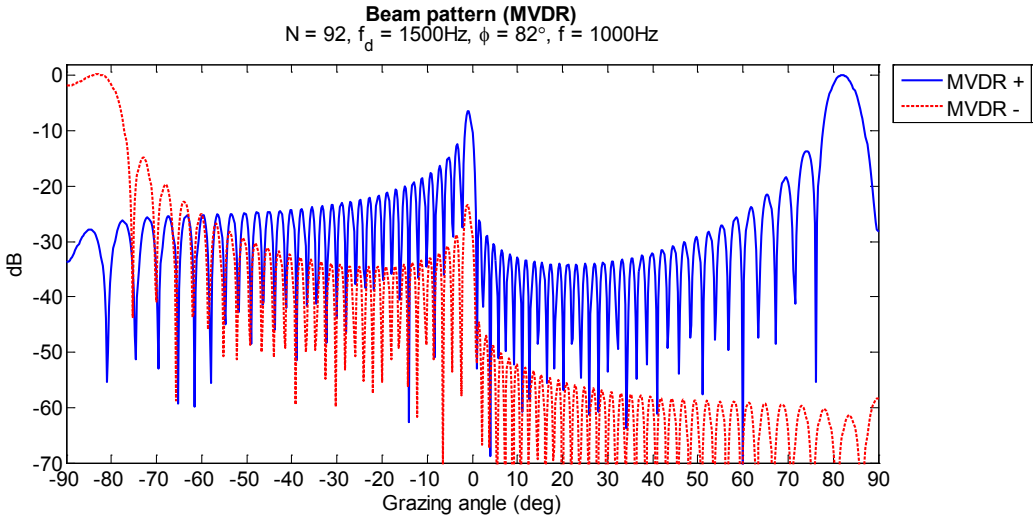

Figure 5: Comparison of the up- (+82°) and down-looking (-82°) MVDR beam patterns in a region where the BL estimate is poor.

A study of the beam patterns showed that in the regions where artifacts are present, the MVDR produces beam patterns having main lobes of markedly different widths for the two directions $\pm\phi$ used to estimate the power reflection coefficient in eq.(2). Figure 5 shows the MVDR beam patterns for the up- and the down-looking steering angles in a region where the BL estimate was poor in Fig.4. Due to the highly asymmetric noise field the MVDR beamformer produces different beams when steered

towards the surface (positive angles) compared to those steered towards the seabed (negative angles). When steering towards the surface, the contribution of the power coming from the bottom is very low due to the bottom loss, so the side lobes in the $\theta < 0$ (down-looking) region do not need to be kept as low. Although this appears to be a desirable behavior, in this case it also produces a negative effect: The two main lobes are markedly different, with the down-looking lobe being significantly wider than the up-looking lobe. Although this does not prevent the MVDR beam former from achieving its power-minimization goal, in this case it disrupts the BL estimation by altering the ratio in eq.(2) to the extent that it no longer represents the ratio of the actual power impinging on the array from the two opposite directions. This main-lobe asymmetry does not occur in regions where the BL estimate is good. The main-lobe asymmetry described above occurs also in regions where the MVDR beam former produces poor BL estimates when applied to the more realistic fields produced by OASN, and its effect is so relevant that in most cases it is possible to relate it to the artifacts in the BL patterns by simply plotting the quantity

$$P_{diff,dB}(|\phi|,f) = 10Log(P(+|\phi|,f)/P(-|\phi|,f), \tag{8}$$

where:

$$P(\phi,f) = \left| \sum_{\theta=-90^\circ}^{+90^\circ} \tilde{\mathbf{w}}^H(\phi,f)\mathbf{a}(\theta,f) \right|^2, \tag{9}$$

(where $\tilde{\mathbf{w}}(\phi,f)$ is the steering vector and θ is the grazing angle of a unit-amplitude plane wave $\mathbf{a}(\theta,f)$ of frequency f). As Fig.6 and Fig.7 show, the regions where $P_{\mathrm{diff,dB}}$ is negative (a circumstance that is directly related to the greater width of the down-looking main lobe) correspond to those where the BL value estimated using MVDR BF is significantly lower than expected.

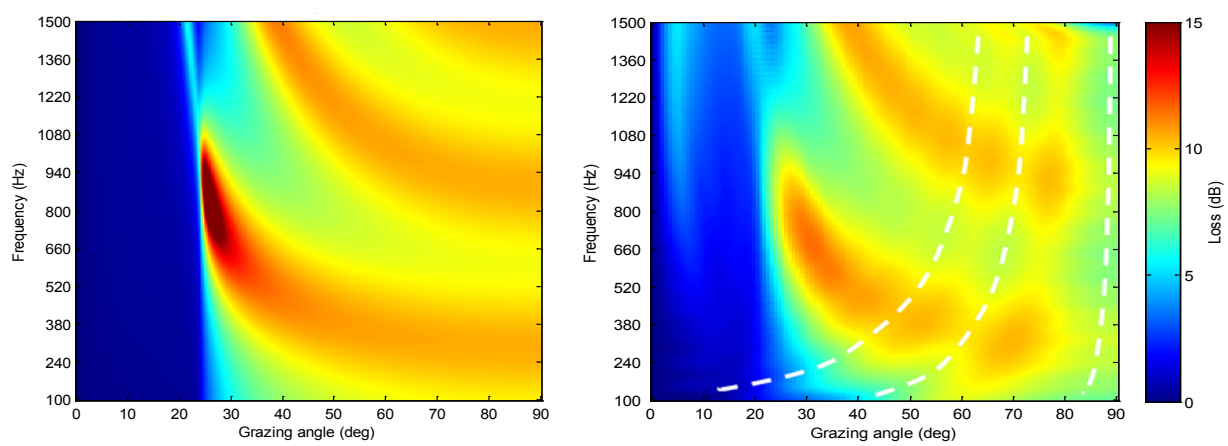

Figure 6: BL pattern obtained by the theoretical model (left) and by applying the MVDR beamformer to the CSD matrix produced by OASN with the same bottom configuration (right). Note the areas of BL disruption occurring in the same regions where the MVDR beam former produced analogous artifacts in the idealized case of Fig.4.

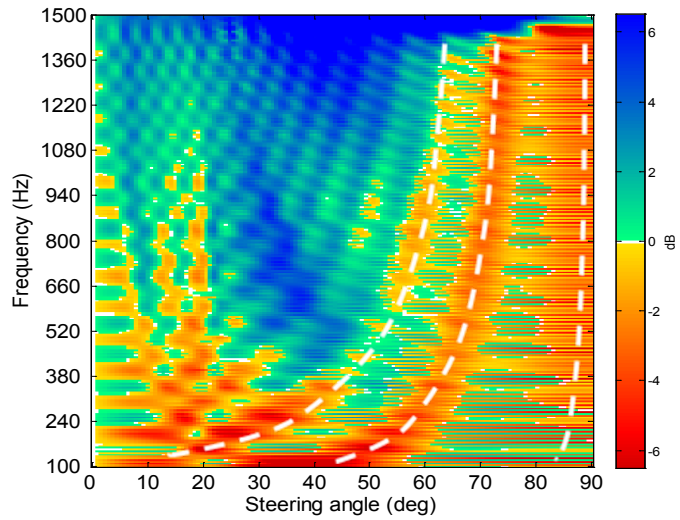

Figure 7: $P_{diff,dB}$ as a function of steering angle and frequency, plotted with the same axis orientation as the BL patterns. Note how the areas of stronger negative minima correspond to the disruptive striations inFig.6.

Interestingly, for the constant-BL case, the BL estimate can be significantly improved by simply removing the asymmetry in the beamformer steering weights. In Fig. 8, the left panel is a slice of the bottom loss curve at 1467 Hz (loss vs. grazing angle) using CBF. Ideally the blue curve would lie on top of the green curve but differs due to the beamformer effects. The middle panel of Fig. 8 shows the MVDR result and the artifacts especially at high grazing angles are evident. In the right panel of Fig. 8, the MVDR results are shown but in this case the downward steered beam is conjugated and used for the upward looking beam. This insures symmetrical beams and for this case significantly improves the bottom loss estimate in comparison to both the proper MVDR and CBF.

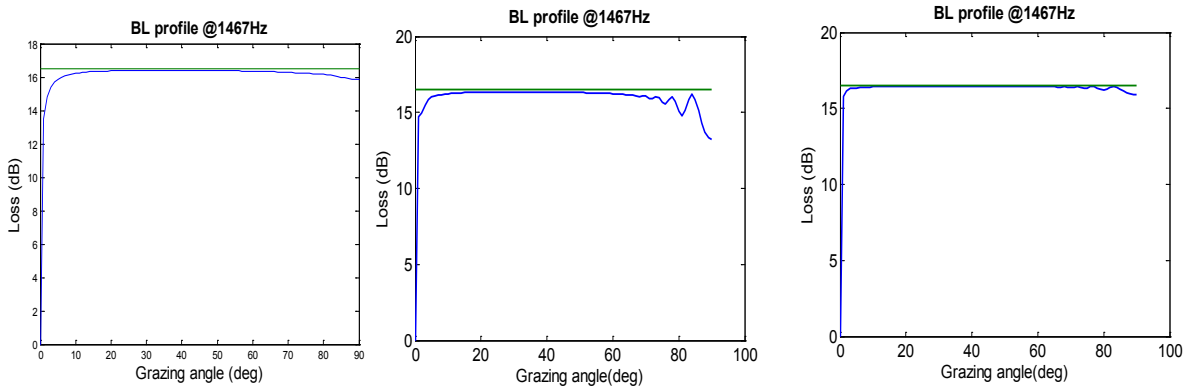

Figure 8: Cross section of the BL profile for the conventional (left), MVDR (center), and MVDR-conjugate (right) beam former.

IMPACT/APPLICATIONS

This work may have a significant impact on several Navy sonar systems (e.g., ASW, MCM, underwater acoustic communications). Knowing the seabed properties will improve at-sea situational

awareness by being able to accurately predict acoustic propagation. And, because this is a passive method it can be designed into a system used for covert activities, low power applications and can be used even in environmentally restricted areas.

TRANSITIONS

Results of this research are being developed under the Ocean Bottom Characterization Initiative (PMW-120). This involves developing a sensor (over the next several years) that is based on techniques described here and will initially be deployed by the Naval Oceanographic Office.

REFERENCES

1. M. Siderius, C.H. Harrison and M. Porter, "A passive fathometer technique for imaging seabed layering using ambient noise", *J. Acoust. Soc. Am*., **120**, 1315-1323, 2006.

2. C.H. Harrison and D.G. Simons, "Geoacoustic inversion of ambient noise: A simple method," *J. Acoust. Soc. Am*., **112**(4), 1377–1389, 2002.

3. J. Arvelo, "Aggressive Adaptive Beamforming for Ambient Noise Inversion with a Limited-Aperture Sonar on an Autonomous Platform", *Proceedings of Meetings on Acoustics* **5**(1), 055003–055003-13, 2008.

4. C.H. Harrison and A. Baldacci, "Bottom reflection properties deduced from ambient noise: simulation of a processing technique", North Atlantic Treaty Organization SACLANT Undersea Research Centre, La Spezia (Italy), Rep. SM392, Nov. 2002.

5. C.H. Harrison, "Performance and limitations of spectral factorization for ambient noise sub-bottom profiling", *J. Acoust. Soc. Am*., **118** (5), 2913–2923, 2005.

6. H. Schmidt, "OASES user's guide and reference manual", MIT Department of Ocean Engineering, 1999.

PUBLICATIONS

1. M. Siderius, H. Song, P. Gerstoft, W. Hodgkiss, P. Hursky and C,.H. Harrison, "Adaptive passive fathometer processing", *J. Acoust. Soc. Am*., **127**, (4), pp. 2193-2200, April 2010 [published, refereed].

2. M. Siderius, "Acoustic remote sensing of the seabed using ambient noise", 2nd International Conference on Shallow Water Acoustics, Sept. 16-20, 2009, Shanghai, China [published in 2010].

3. J. Gebbie, M. Siderius, L. Muzi, J. Paddock, "Extracting the Rayleigh reflection coefficient from the passive fathometer", OCEANS 2010, MTS/IEEE Seattle, 20–23 Sep. 2010 [published, refereed].

4. L. Muzi, M. Siderius, J. Gebbie, J. Paddock, “On the use of adaptive beam-forming techniques for geoacoustic inversion of marine ambient noise”, OCEANS 2010, MTS/IEEE Seattle, 20–23 Sep. 2010 [published, refereed].